PHYSICAL REVIEW E **73**, 025401(R) (2006)

Nonlinear development of stimulated Raman scattering from electrostatic modes excited by self-consistent non-Maxwellian velocity distributions

L. Yin,[1] W. Daughton,[1,2] B. J. Albright,[1] B. Bezzerides,[1] D. F. DuBois,[1] J. M. Kindel,[1] and H. X. Vu[3]
[1]*Los Alamos National Laboratory, Los Alamos, New Mexico 87545, USA*
[2]*Department of Physics and Astronomy, University of Iowa, Iowa City, Iowa 52242, USA*
[3]*University of California, San Diego, California 92093, USA*
(Received 24 November 2004; published 10 February 2006)

The parametric coupling involving backward stimulated scattering of a laser and electron beam acoustic modes (BAM) is described as observed in particle-in-cell (PIC) simulations. The BAM modes evolve from Langmuir waves (LW) as the electron velocity distribution is nonlinearly modified to be non-Maxwellian by backward stimulated Raman scattering (BSRS). With a marginal damping rate, BAM can be easily excited and allow an extended chirping in frequency to occur as later SRS pulses encounter modified distributions. Coincident with the emergence of this non-Maxwellian distribution is a rapid increase in BSRS reflectivities with laser intensities. Both the reflectivity scaling with laser intensity and the observed spectral features from PIC simulations are consistent with recent Trident experiments.

DOI: 10.1103/PhysRevE.73.025401 PACS number(s): 52.35.Fp, 52.35.Mw, 52.38.Bv, 52.38.Dx

Recent single-hot-spot experiments at the LANL Trident facility have been performed to understand the physics of backward stimulated Raman scattering in a single speckle of a random phase plate smoothed beam [1,2]. The reported data show a rapid increase in backward stimulated Raman scattering (BSRS) with the laser drive intensity in a moderately large $k\lambda_D$ regime (0.33–0.35, where k is the Langmuir wave number and λ_D is the plasma Debye length). In Fig. 1 (triangles), the reflectivity rises steeply from 0.001% to 1% at low intensities ($1.5-2.5\times10^{15}$ W/cm^2) and saturates at 5–10% for higher intensities. In Fig. 1 the reflectivity from one-dimensional (1D) full particle-in-cell (PIC) simulations (details below) exhibits the same rapid onset and saturation of BSRS. The calculated reflectivity shows a steep rise by orders of magnitude to ~1% at 1.1×10^{15} W/cm^2 and saturates at a few percent at higher intensities. These features are in good agreement with reflectivities observed in the Trident experiments. The reflectivity at low intensity, including the steep transition, is comparable to experimental values, a result achieved only by using a much larger number of particles per simulation cell [3] than in previous studies.

While additional effects not included in the simple 1D PIC model need to be examined to fully understand the experimental results, PIC simulations of stimulated Raman scattering (SRS) reflectivity scaling with laser intensity in other parameter regimes ($k\lambda_D$=0.24 to 0.45) show similar interesting features (details discussed elsewhere). This commonly occurring feature motivates us to examine, as a first step, the Thomson scattering spectra associated with the reflectivity scaling with laser intensity. We will forego an attempt here to fully explain the experimental scaling. To this end, a set of simulations for laser intensities ranging from $I_0=8\times10^{14}$ to 1×10^{16} W/cm^2 are performed for $k\lambda_D=0.34$. The fully kinetic PIC simulations use a well-known algorithm in which the fields are advanced using scalar and vector potentials [4]. The simulation domain is 100 μm in length (comparable to the length of a $f/4.5$ diffraction limited beam) with 1000 particles per cell for each species [3]. A 527-nm laser enters from the left boundary. The simulated plasma has T_e=700 eV, T_i=140 eV, n_e/n_{cr}=0.036 and cell size $0.75\lambda_D$, parameters chosen to mimic the plasma conditions in the Trident experiment [1,2]. The laser drive is spatially uniform and open boundary conditions are used for the fields [5] and particles. Results from these runs show the growth of BSRS at early times, however, it is suppressed later by the growth of stimulated Brillioun scattering (SBS). To maintain a longer period of active BSRS, SBS is disabled by fixing the ions. Reduced PIC (RPIC) [6] and full PIC results show that BSRS saturation involving the Langmuir decay instability (LDI) is not energetically significant in this parameter regime. The Trident experiments, that involve physics not included in our simple 1D model [2,7], do not measure strong SBS signals.

We first examine high intensity runs with $I_0=5\times10^{15}$ to 1×10^{16} W/cm^2 (the last three points on the plateau in Fig. 1). Each run exhibits a large growth of BSRS, a few hundred $\omega_{pe}t$ after the laser has traversed the simulation domain. The inset in Fig. 1 shows time-averaged reflectivity as a function of time for $I_0=5\times10^{15}$ W/cm^2 (solid curve).

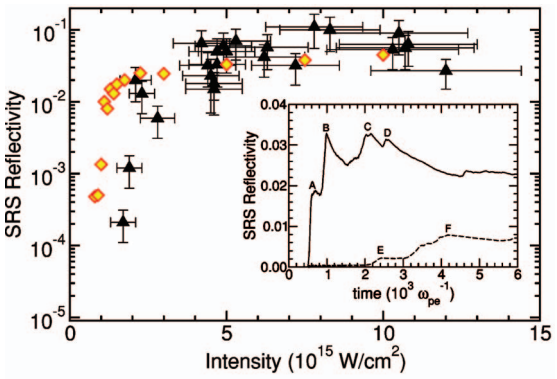

FIG. 1. (Color) Time-averaged reflectivities from Trident single-speckle experiments (triangles) [1] and from PIC simulations (diamonds: averaged over time $\omega_{pe}t$=6000). Also shown in the inset are the time-averaged reflectivities from simulations for intensities $I_0=5\times10^{15}$ W/cm^2 (solid curve) and $I_0=1.2\times10^{15}$ W/cm^2 (dashed curve).

During $\omega_{pe}t=0-3000$, four large peaks (labeled *A* through *D*) are seen in the reflectivity curve. The electrostatic (ES) wave spectrum $|E_x(k,\omega)|^2$ during this time [shown by the color contours in Fig. 2(a)] shows that the enhancement in energy occurs on a pronounced "streak" [7,8] that begins with ω and k intersecting the Langmuir branch (long-dashed curve). The streak exhibits a large downshift in ω (about $0.5\omega_{pe}$) with a very narrow increase in k, a feature similar to that observed in the Trident experiments [2,9]. The spectra for intervals $\omega_{pe}t=500-800$ (for peak labeled *A* in the inset of Fig. 1), 800–1200 (*B*), 1800–2300 (*C*), and 2400–2800 (*D*) have been examined separately; the streak consists of a sequence of four steps in decreasing frequency that correspond to the four backscattering peaks [the four steps appear in the second harmonic spectrum seen in the upper right corner of Fig. 2(a)]. Detailed examination of the electron phase space orbits during the first episode of intense backscattering (*A*) shows clear trapping as well as the appearance of bump-on-tail distributions, as shown by the lower inset in Fig. 2(a) at $\omega_{pe}t=596$ averaged over $x=250-750\lambda_D$. The electron phase space distribution (v_x^e vs x) at this time is displayed in (d). More commonly, F_e (at later times and/or different locations) takes the form of a flat distribution, as shown by the upper inset in Fig. 2(a). Although these distributions were obtained at a given time, they represent averaged features persisting during each reflectivity pulse.

The spatially averaged distribution F_e (over many ES wavelengths) from the simulation and linear stability theory are used to identify the ES modes supported by the plasma. In Fig. 2, the dispersion curves [real frequencies displayed in Fig. 2(a) and imaginary parts in Fig. 2(c)] are numerical solutions to the general dispersion relation for stimulated scattering of a pump electromagnetic wave into electrostatic and electromagnetic modes [10]. Neglecting ion response ($\omega \gg \omega_{pi}$), $2(1+\chi_e)D_-(\omega,k)+k^2v_o^2\chi_e=0$. Here $D_-(\omega,k)\equiv\omega^2-2\omega\omega_0-c^2(k^2-2kk_0)$, ω_0 and k_0 are the frequency and wave number of the pump wave, ω and k are the frequency and wave number of the ES wave, v_o is the electron quiver velocity, and χ_e is the electron susceptibility calculated from F_e shown in the lower inset of Fig. 2(a). The non-Maxwellian F_e results in the excitation of ES waves that are on the electron beam acoustic mode (BAM) branch [11]. The dotted curves are for an unstable root (BAM1), while the dash-dotted curves are for a stable root (BAM2) at this stage. There are infinite number of BAM roots between BAM1 and BAM2 whose phase velocities are in the range of $\simeq 2.8-5v_{th}^e$ in the non-Maxwellian tail of the distribution, as shown in the inset in Fig. 2(b). In the subsequent discussion, we focus on BAM within the velocity range and the role of BAM in the nonlinear development of SRS {stimulated electron acoustic wave scattering (SEAS) associated with a much lower phase velocity $1.4\pm0.08v_{th}^e$ is also observed in the backscattered light spectrum in experiments [1]; see also related theoretical and simulations studies [12]}. The real frequencies of BAM1 and BAM2 are almost identical to the modes for $v_o=0$. However, in the presence of the parametric coupling a growing mode arises [with frequencies and growth rates shown by the solid curves in Figs. 2(a) and 2(c), respectively]. The simulation indicates that for an initially Maxwellian plasma ($\omega_{pe}t\leqslant 400$) the laser drive excites very low level BSRS and ES waves that intersect the Langmuir branch. The growth rate for the parametric coupling peaks around $k\lambda_D\simeq 0.34$, consistent with the k value where the streak in the simulation intersects the Langmuir branch.

In contrast, large backscattering occurs for the wave-modified electron distribution at $\omega_{pe}t>500$. The BAM are unstable with little contribution from parametric coupling in the region of $k\lambda_D=0.1-0.3$. Comparing the enhanced spectral power in red in (a) and the linear solution (c), the latter clearly outlines this region of observed enhanced spectral activity. A region of growth exists [solid curve in (c)] in which the large $\delta\omega$ ($\sim 0.5\omega_{pe}$) and the narrow δk coincide with those of the streak in (a) obtained from simulation, a direct result of the parametric coupling. In this region the linear solution is dominated by the zeros of D_- with the result that the modes excited satisfy the frequency matching condition for the backscattered light $(\omega-\omega_0)^2-\omega_{pe}^2=(k-k_0)^2c^2$ [8]. The streak aligns with this locus of modes. The electromagnetic wave spectrum $|E_y(k,\omega)|^2$ in panel (b) reveals that the ES spectral streak is matched to the BSRS streak with an increase in ω (about $0.5\omega_{pe}$) over a narrow $-k$ range (for the incident laser, $k\lambda_D\simeq 0.19$). The slope of the streak in the linear solution matches the group velocity of the BSRS scattered light wave [8]. Note for the bump-on-tail distribution BAM1 is a damped mode in the streak region of parametric resonance with damping comparable to the Landau damping of the usual BSRS matched Langmuir waves (LWs). However, a flat electron distribution similar to that shown in the inset of Fig. 2(a) is more commonly seen in the middle spatial region during subsequent pulses. Linear dispersion solutions reveal that the damping rate of BAM2 at the matching k (with a lower frequency) evolves to marginal stability as the distribution changes from bump on tail to flat as shown in red in Fig. 2(c). This result suggests that the weakly damped BAM modes can be in parametric resonance and are easily excited by the spectral streaking, consistent with the increasingly larger reflectivity obtained for the subsequent pulses (*B*, *C*, and *D*) shown in inset of Fig. 1 as the frequency downshift continues. Taken as a whole, results of the simple linear stability analysis outlined above agree with the spectra present in simulations.

The highest ω and lowest k modes grow to large amplitude first, followed by subsequent growth of ES waves at lower frequencies. As the first BSRS pulse travels toward the laser at high group velocity ($\simeq 0.95c$), it generates ES waves and hot electrons. When the backscattered light pulse exits the left boundary, the ES waves and hot electrons move in the laser direction with speed $\simeq 2.8-5v_{th}^e$. The BSRS matching conditions for the second backscattered pulse start at new ω (k) values lower (higher) than those for the previous pulse, and similarly for the third and fourth pulses. The extended locus of the streak observed in the time interval $\omega_{pe}t=400-3000$ is actually a sequence of frequency downshifts or chirps, each point of origin in frequency set by the modified background conditions residual to the previous pulse. Similarly, the ES k spectrum as a function of time shows the initial k values of successive pulses do not return to the initial matched value [7]. As this process develops, the primary

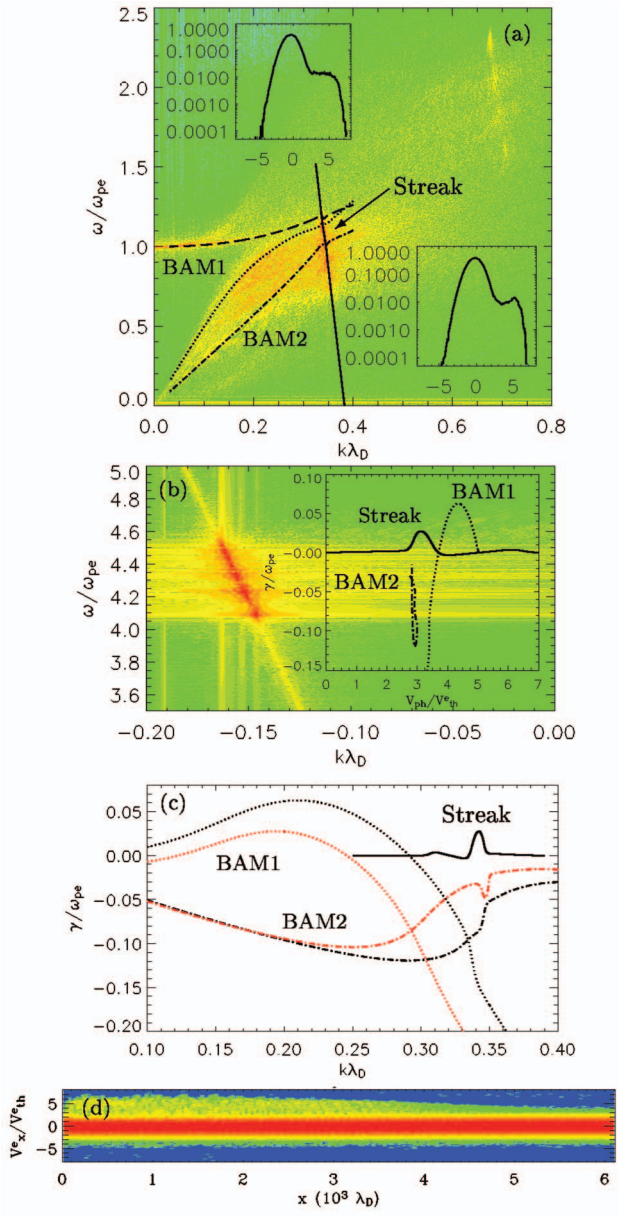

FIG. 2. (Color) Results of SRS simulation and linear dispersion for a strong drive $I_0=5\times10^{15}$ W/cm^2: Panel (a) shows a logarithmic plot of ES wave energy in color. Overlaid are linear dispersion curves for the ES modes: streak (solid), Langmuir (dashed), unstable (dotted; BAM1) and stable (dash-dot; BAM2) BAM. The lower inset shows a bump-on-tail electron distribution present during the peak of the first reflectivity pulse. The upper inset is a representative flat distribution more commonly seen in the middle spatial region during subsequent pulses. Panel (b) is the electromagnetic spectrum; excitation of BSRS starts at the matching condition and continues to higher frequencies. The inset is the growth rate vs the wave-phase velocity for the ES modes using a bump-on-tail distribution. Panel (c) shows growth rates of the two BAM (black and red curves for bump-on-tail and flat distributions, respectively) and the streak (solid). BAM1 (dotted) exhibits strong growth, as does the streak. Panel (d) shows electron-phase space at $\omega_{pe}t=596$ during the first episode of strong BSRS. A non-Maxwellian tail is evident where backscattered light grows to large amplitude.

ES waves coupled to the backscattered light have ω and k that intersect the domain of BAM not LW activity. This range of decreasing frequency is populated by BAM modes of decreasing damping rates as the non-Maxwellian tail becomes more flat. Strong parametric coupling and gain are highly localized to the location of the reflected light pulse as it translates towards the entrance boundary of the incident light wave. These results show that the nonlinear (NL) development of BSRS is a complex spatial-temporal process [8] involving the evolution of a non-Maxwellian distribution, excitation of BAM, and the coupling intrinsic to the parametric instability.

Near the transition at lower intensity, the behavior is different. We consider here representative results for $I_0=1.2\times10^{15}$ W/cm^2. The reflectivity time history, displayed in inset of Fig. 1 by the dashed curve, shows that the first significant enhancement occurs later in time than for high intensities (solid curve) since a longer time is needed for BSRS to modify the electron distribution significantly. In the initial phase $\omega_{pe}t<2000$, the electron distribution is near Maxwellian and LWs couple to BSRS. Later, at the time of peak E, the electrons at the left of the simulation domain are non-Maxwellian and the ES waves that couple to the first large backscattered pulse are the BAM, though the growth for the parametric coupling occurs in a narrower region in ω and k than in the high intensity cases. As pulse E leaves the system, a streak narrow in ω intersects the BAM. Again, linear dispersion roots using the non-Maxwellian distribution from simulation agree with spectral modes present in simulation. Pulse F then amplifies to a larger amplitude in a plasma with hot electrons and BAM produced by pulse E. Generally, in runs with reflectivity $\geqslant1\%$, large backscatter of the light pulses are associated with parametric coupling to BAM, not LW. However, the spectral lengths of the streak $\delta\omega$ are shorter in the lower intensity runs than in the strong drive cases.

Lowering the laser intensity beneath the threshold ($I_0\leqslant1\times10^{15}$ W/cm^2) leads to an observed reflectivity well below 1%. The electron distribution then remains essentially Maxwellian and BAM is absent. A spectral streak very narrow in ω is identified intersecting the Langmuir branch as the frequency shifts downward due to trapping [6,7].

We note that the dynamics in the BSRS simulations reported here is in accord with earlier work in that the reflected light consists of a series of subpicosecond pulses [6]. The NL behavior involves a balance between reduction of the Landau damping and detuning of the parametric frequency resonance due to the frequency shift from electron trapping. The spectral streaks are a direct result of the chirping of the frequency shift and the modification of the distribution function as the reflected light pulses rise and fall in amplitude. This chirping cannot be described by a steady-state saturation model. In previous studies of this parameter regime, electron trapping and the NL frequency shift were considered as the primary NL saturation mechanism [6] (see as well Ref. [13]). A three-wave model was introduced [6] describing the evolution of the envelopes of the laser, the scattered light, and the ES wave, with the NL frequency shift determined to be the primary saturation mechanism. The frequency shift was assumed to scale with local-in-space-and-time bounce fre-

quency through a constant scale factor. All known (e.g., Ref. [14]) theoretical formulas for this frequency shift take this form with the scale factor given as a function of the background velocity distribution, specifically the second derivative. This scale factor shows a fivefold decrease for the distribution function shown in Fig. 2(a) over its Maxwellian counterpart. Three-wave model studies routinely show that a modest change in the scale factor implies a proportionally much larger change in the time-average reflectivity. Indeed, the fivefold decrease of the scale factor for the distribution function of Fig. 2 would result in a jump in the time-average reflectivity over that of a Maxwellian by orders of magnitude.

In earlier 1D simulations [6], side loss was found to raise the threshold for reflectivity. Noting that for weak drive the background distribution returns to Maxwellian, one may infer that the steep rise in reflectivity with laser intensity is a direct result of the NL modified background distribution function through the frequency shift. As a test, a process that restores the distribution to Maxwellian should shift the threshold for reflectivity onset to higher drive strengths. This was verified within 1D simulations by comparing results with and without side loss.

We acknowledge useful discussions with D. Barnes, E. Dodd, J. Fernández, N. Hoffman, J. Kline, D. Montgomery, and H. Rose. This work was performed under the auspices of the U.S. DOE by the University of California, Los Alamos National Laboratory, under Contract No. W-7405-Eng-36.

[1] D. S. Montgomery *et al.*, Phys. Plasmas **9**, 2311 (2002).

[2] J. L. Kline *et al.*, Phys. Rev. Lett. **94**, 175003 (2005).

[3] Shortening the simulation length and including the side loss of hot electrons in 1D (Ref. [6]) and two-dimensional (2D) simulations will raise intensity value at the onset and improve the agreement. However, qualitative spectral properties discussed in this work, one of our main concerns, are insensitive to the exact simulation length, as confirmed by 70 μm simulations. While convergence of the results were verified by 4000 particles per cell runs, 32 particles per cell shows onset at much higher intensity and has lower saturation level, both inconsistent with Trident results.

[4] W. Daughton *et al.*, J. Geophys. Res. **106**, 25031 (2001).

[5] C. W. Neilson and E. L. Lindman, Proceedings of the Sixth Conference on Numerical Simulation of Plasmas, Berkeley, CA, 1973 (unpublished), pp. 148–151.

[6] H. X. Vu, D. F. DuBois, and B. Bezzerides, Phys. Rev. Lett. **86**, 4306 (2001); Phys. Plasmas **9**, 1745 (2002).

[7] Supersonic transverse flow and longitudinal thermal gradients caused by collision-induced inhibited thermal conductivity can reduce Brillioun Scattering (SBS) by one to two orders of magnitude [D. F. DuBois, H. X. Vu, and B. Bezzerides, Workshop on SRS/SBS Saturation at Wente Vineyards, Livermore, CA, 2002 (unpublished), Report No. UCRL-JC-14893-SUM.

[8] H. X. Vu, L. Yin, D. F. DuBois, B. Bezzerides, and E. S. Dodd, Phys. Rev. Lett. **95**, 245003 (2005).

[9] The spectral width of the streak from simulations is larger than was measured at Trident in part because the simulations omit some effects present in the experiment (see Ref. [2]). In 2D PIC simulations, BAM dispersion remains essentially the same but the streak has a narrower frequency shift which is closer to that seen in the Trident experiments. We emphasize that the spectral features seen in experiments and simulations are similar, though not necessarily in quantitative agreement.

[10] J. F. Drake *et al.*, Phys. Fluids **17**, 778 (1974); D. W. Forslund, J. M. Kindel, and E. L. Lindman, *ibid.* **18**, 1002 (1975).

[11] T. M. O'Neil and J. H. Malmberg, Phys. Fluids **11**, 1754 (1968); L. Yin *et al.*, J. Geophys. Res. **103**, 29595 (1998).

[12] H. A. Rose and D. A. Russell, Phys. Plasmas **8**, 4784 (2001); Lj. Nikolic *et al.*, Phys. Rev. E **66**, 036404 (2002); B. Afeyan *et al.*, Third International Conference on Inertial Fusion Sciences and Applications (IFSA 2003), Monterey, CA, 2003 (American Nuclear Soc. Inc., La Grange, IL,2004), p. 213.

[13] S. Brunner and E. J. Valeo, Phys. Rev. Lett. **93**, 145003 (2004). The authors proposed a saturation mechanism which could also be operative based on the trapped particle instability.

[14] G. J. Morales and T. M. O'Neil, Phys. Rev. Lett. **28**, 417 (1972); H. A. Rose and D. A. Russell, Phys. Plasmas **8**, 4784 (2001).